

IMAGE MODELING AND RESTORATION BY HIGHER-ORDER STATISTICS BASED INVERSE FILTERS

Chien-Chung Hsiao and Chong-Yung Chi

Department of Electrical Engineering
National Tsing Hua University
Hsinchu, Taiwan, Republic of China

ABSTRACT

This paper presents image modeling and restoration by higher-order statistics based 2-D inverse filters. A given original image $x(m, n)$ is processed by an optimum inverse filter $v(m, n)$ which is designed by maximizing cumulant based criteria $J_{r,m} = |C_m|^r / |C_r|^m$ where r is even, $m > r \geq 2$ and C_m (C_r) denotes m th-order (r th-order) cumulant of the output $e(m, n)$ of the 2-D inverse filter. The original image $x(m, n)$ can be modeled as the output of a linear shift-invariant (LSI) system $h(m, n)$ driven by $e(m, n)$ where $h(m, n)$ is a stable inverse filter of $v(m, n)$. When a blurred image $y(m, n) = x(m, n) * g(m, n)$ rather than the original image $x(m, n)$ is given, $x(m, n)$ can be restored by first estimating $e(m, n)$ using the previous inverse filter criteria and then obtain $x(m, n) = e(m, n) * h(m, n)$. Some experimental results are provided to support the proposed image modeling and restoration method.

1. INTRODUCTION

Assume that $x(n)$ is the non-Gaussian output signal of an unknown linear shift-invariant (LSI) system $h(n)$ driven by an independent identically distributed (i.i.d.) non-Gaussian random signal $u(n)$. Cumulant based inverse filter criteria [1-4] maximizing $J_{r,m}(v(n)) = |C_m|^r / |C_r|^m$ with admissible r and m have been considered for the estimation of the inverse filter $v(n)$ of the unknown LSI system $h(n)$ where C_m denotes the m th-order cumulant of the output signal $e(n)$ of the inverse filter $v(n)$ with input $x(n)$.

Tugnait [5] extended the above criteria $J_{2,3}$, $J_{2,4}$ and $J_{4,6}$ [3] to the 2-dimensional (2-D) case for estimation of ARMA parameters of an unknown 2-D LSI system with only non-Gaussian output $x(m, n)$ of the system, and he [6] also proposed a texture synthesis method using these 2-D inverse filter criteria.

In this paper, we theoretically show that the above criteria $J_{r,m}$, which only use two cumulants, for the 2-D case are applicable only for r being even and $m > r \geq 2$. These criteria for admissible values of r and m can be applied to image modeling and restoration [7,8], by treating images as the output of a 2-D LSI system driven by a 2-D non-Gaussian random

field. Some experimental results for image modeling and restoration using these inverse filters and a 2-D correlation based prediction error method [9] are provided. Finally we draw some conclusions.

2. TWO-DIMENSIONAL CUMULANT BASED INVERSE FILTERS

Assume that the given 2-D measurements $x(m, n)$, $m = 0, 1, \dots, N-1$, $n = 0, 1, \dots, N-1$ are generated from the following convolutional model:

$$x(m, n) = u(m, n) * h(m, n) + w(m, n) \quad (1)$$

with the following assumptions:

- (A1) $h(m, n)$ is an LSI stable system and a stable inverse system $h_I(m, n)$ of $h(m, n)$ exists.
- (A2) The driving input $u(m, n)$ is real, zero-mean, i.i.d., non-Gaussian with m th-order cumulant γ_m where $m \geq 3$.
- (A3) The measurement noise $w(m, n)$ is Gaussian with unknown statistics.
- (A4) $u(m, n)$ and $w(m, n)$ are statistically independent.

Assume that $v(m, n)$ is a stable 2-D inverse filter estimate for $h_I(m, n)$. Let

$$e(m, n) = x(m, n) * v(m, n) \quad (2)$$

The cumulant based inverse filter criteria using two cumulants of $e(m, n)$ with different cumulant orders are described in the following Theorem:

Theorem 1. Assume that $x(m, n)$ is generated from the model given by (1) under the previous assumptions (A1) through (A4). Let

$$J_{r,m}(v(m, n)) = \frac{|C_m|^r}{|C_r|^m} \quad (3)$$

where C_m (C_r) denotes the m th-order (r th-order) cumulant of $e(m, n)$ given by (2). Then the following statements are true:

(S1) $J_{r,m}(v(m,n))$ is bounded only if $r = 2s$ (i.e., r is even), $m = l+s > r$ where $l > s \geq 1$. Moreover,

$$\max \{J_{2s,l+s}(v(m,n))\} = \frac{|\gamma_{l+s}|^{2s}}{|\gamma_{2s}|^{l+s}} \quad (4)$$

(S2) The optimum $\hat{v}(m,n)$ associated with $J_{2s,l+s}(v(m,n)) = \max \{J_{2s,l+s}(v(m,n))\}$ where $l > s \geq 1$ satisfies

$$\hat{v}(m,n) * h(m,n) = \alpha \delta(n - \tau_1, m - \tau_2), \quad (5)$$

where $\alpha \neq 0$ is a scale factor and τ_1 and τ_2 are unknown integers, for the case that $s = 1$ and $SNR = \infty$ and the case that $s > 1$ and SNR is finite.

Chi and Wu [2] have shown this theorem for 1-D case. The proof of this theorem for 2-D case follows the same procedure as that for 1-D case.

In practice, cumulants C_m and C_r in $J_{r,m}$ given by (3) must be replaced by the corresponding sample cumulants, and the associated inverse filter $v(m,n)$ can be assumed to be an FIR filter. Because $J_{r,m}$ is a highly nonlinear function of $v(m,n)$, one has to resort to iterative optimization algorithms to estimate the coefficients of $v(m,n)$. The associated optimum $e(m,n)$ is then an estimate for the driving input $u(m,n)$.

3. APPLICATION OF INVERSE FILTERS TO IMAGE MODELING

Assume that $x(m,n)$ is an original image which is modeled as (1) where $w(m,n) = 0$ and $h(m,n)$ is a causal AR system, i.e., $x(m,n)$ can be expressed as

$$\begin{aligned} x(m,n) &= u(m,n) * h(m,n) \\ &= \sum_{k=0}^p \sum_{\substack{l=0 \\ (k,l) \neq (0,0)}}^p a(k,l) x(m-k, n-l) + u(m,n) \end{aligned} \quad (6)$$

which implies that the inverse filter $h_I(m,n) = a(m,n)$ of $h(m,n)$ is a $(p+1) \times (p+1)$ causal FIR filter with region of support $S = \{(m,n) \mid 0 \leq m \leq p, 0 \leq n \leq p\}$. Therefore, the optimum inverse filter $\hat{v}(m,n)$ associated with $J_{r,m}$ can be used as an estimate for the AR model coefficients $a(m,n)$ of the image. Next, let us show an example for image modeling.

Example 1. An 128×128 image shown in Figure 1(a) was processed by the optimum inverse filter associated with $J_{2,3}$ assuming that the inverse filter $v(m,n)$ is a 3×3 causal FIR filter. The processed image is shown in Figure 1(b) and the AR parameters $\hat{a}(m,n)$ are shown in Table 1. One can see, from Table 1 and Figures 1(a) and 1(b), that the obtained AR model coefficients $\hat{a}(m,n)$ of the image are quite close to $\delta(m,n)$ which accounts for the similarity of these two images.

4. APPLICATION OF INVERSE FILTERS TO IMAGE RESTORATION

Assume that the original image $x(m,n)$ is blurred by an LSI system and the blurred image $y(m,n)$ is given by

$$\begin{aligned} y(m,n) &= x(m,n) * g(m,n) \\ &= u(m,n) * (h(m,n) * g(m,n)) \end{aligned} \quad (7)$$

Let $v(m,n)$ be the inverse filter of the system $h(m,n) * g(m,n)$ associated with the blurred image $y(m,n)$ and $\hat{v}(m,n)$ be the associated optimum cumulant based inverse filter. Assuming that the image model $h(m,n)$ is known, the restored image can be obtained by

$$\hat{x}(m,n) = y(m,n) * \hat{v}(m,n) * h(m,n) \quad (8)$$

which means that the optimum restoration filter is given by $\hat{v}(m,n) * h(m,n)$. In other words, the image restoration can be performed without need of any knowledge about the blurred system but the image model must be given in advance. Next, let us show some experimental results for image restoration.

Example 2. The original image $x(m,n)$ shown in Figure 1(a) was also used in this example. Three cases for the blurred system $G(z_1, z_2)$ are considered:

Case 1: $G(z_1, z_2)$ is a 3×3 causal FIR filter

$$\begin{aligned} G(z_1, z_2) &= 1 + \frac{1}{8}z_1^{-1} + \frac{1}{8}z_2^{-1} + \frac{1}{8}z_1^{-2} + \frac{1}{8}z_1^{-1}z_2^{-1} \\ &\quad + \frac{1}{8}z_2^{-2} + \frac{1}{8}z_1^{-2}z_2^{-1} + \frac{1}{8}z_1^{-1}z_2^{-2} + \frac{1}{8}z_1^{-2}z_2^{-2} \end{aligned} \quad (9)$$

Case 2: $G(z_1, z_2)$ is an allpass filter

$$G(z_1, z_2) = \frac{9 + 2z_1^{-1} - 3z_2^{-1} + z_1^{-1}z_2^{-1}}{1 - 3z_1^{-1} + 2z_2^{-1} + 9z_1^{-1}z_2^{-1}} \quad (10)$$

Case 3: $G(z_1, z_2)$ is a causal AR filter

$$G(z_1, z_2) = \frac{1}{1 - 0.5z_1^{-1} - 0.3z_2^{-1} + 0.15z_1^{-1}z_2^{-1}} \quad (11)$$

Again, the inverse filter criteria $J_{2,3}$ was used to obtain the optimum inverse filter $v(m,n)$ which was assumed to be a causal FIR filter.

For **Case 1**, the blurred image is shown in Figure 2(a). The inverse filter was assumed to be a 5×5 causal FIR filter. The restored image obtained by the optimum inverse filter associated with $J_{2,3}$ is shown in Figure 2(b). For comparison, the restored image obtained by the 2-D correlation based prediction error method [9] is also shown in Figure 2(c). One can see that the restored image shown in Figure 2(b) is much better than the one shown in Figure 2(c).

For **Cases 2 and 3**, the inverse filter was assumed to be a 7×7 causal FIR filter and a 5×5 causal FIR filter, respectively. The results corresponding to those shown in Figures 2(a) through 2(c) are shown

in Figures 3(a) through 3(c) for Case 2 and Figures 4(a) through 4(c) for Case 3, respectively. The same conclusion as drawn from Case 1 also applies for these two cases.

5. CONCLUSIONS

The applications of cumulant based inverse filter criteria $J_{2s,l+2}$ given by (3) where $l > s \geq 1$ to image modeling and restoration have been presented. The image restoration can be performed without need of any knowledge about the blurred system but the image model must be given in advance. Some experimental results are provided to illustrate these applications. However, the original image and the blurred systems used in the experiment have broadband spectra. The case that either the image or the blurred system does not have a broadband spectrum is still under study.

ACKNOWLEDGMENTS

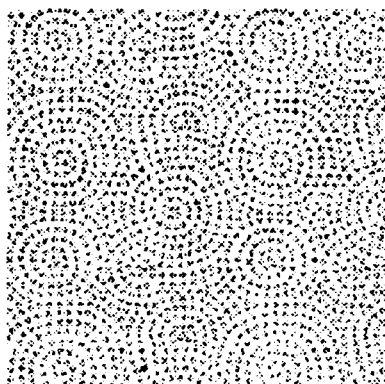
This research was supported by the National Science Council under Grant NSC-83-0404-E-007-037.

REFERENCES

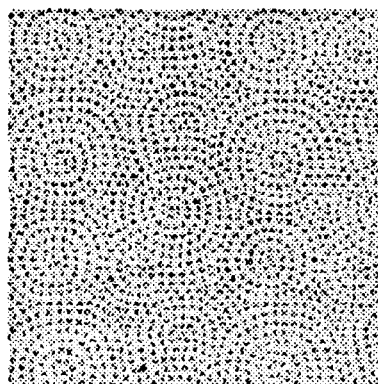
- [1] R. A. Wiggins, "Minimum entropy deconvolution," *Geoexploration*, vol. 16, pp. 21-35, 1978.
- [2] C.-Y. Chi and M.-C. Wu, "Inverse filter criteria for blind deconvolution and equalization using two cumulants," submitted to *Signal Processing*.
- [3] J. K. Tugnait, "Estimation of linear parametric models using inverse filter criteria and higher-order statistics," *IEEE Trans. Signal Processing*, vol. 41, no. 11, pp. 3196-3199, Nov. 1993.
- [4] O. Shalvi and E. Weinstein, "New criteria for blind deconvolution of nonminimum phase systems (channels)," *IEEE Trans. Information Theory*, vol. 36, pp. 312-321, March 1990.
- [5] J. K. Tugnait, "Estimation of linear parametric models of non-Gaussian discrete random fields," in *Image Processing Algorithms and Techniques II*, M. R. Civanlar, S. K. Mitra, R. J. Moorhead II, Editors, Proc. SPIE 1452, 1991, pp. 204-215.
- [6] J. K. Tugnait, "Texture synthesis using asymmetric 2-D noncausal AR models," *Proc. IEEE Signal Processing Workshop on Higher-Order Statistics*, June 1993, pp. 71-75.
- [7] A. K. Jain, "Advances in mathematical models for image processing," *Proc. IEEE*, vol. 69, no. 5, pp. 502-528, May 1981.
- [8] A. K. Jain, *Fundamentals of Digital Image Processing*, Prentice-Hall, Englewood Cliffs, New Jersey, 1989.
- [9] Steven M. Kay, *Modern Spectral Estimation*, Prentice-Hall, Englewood Cliffs, New Jersey, 1988.

Table 1. AR model coefficients $\hat{a}(m, n)$ of the image shown in Figure 1(a) (obtained from the optimum inverse filter associated with $J_{2,3}$).

| $\hat{a}(m, n)$ | | | |
|-----------------|---------|---------|---------|
| | $n = 0$ | $n = 1$ | $n = 2$ |
| $m = 0$ | 1.0000 | -0.0951 | 0.0586 |
| $m = 1$ | -0.1114 | 0.0513 | -0.0003 |
| $m = 2$ | 0.0565 | -0.0033 | 0.0101 |



(a)



(b)

Fig. 1. Experimental results associated with Example 1. (a) The original image $x(m, n)$ (128×128); (b) the processed image $\hat{u}(m, n)$ (input of the AR image model) by the optimum inverse filter associated with $J_{2,3}$.

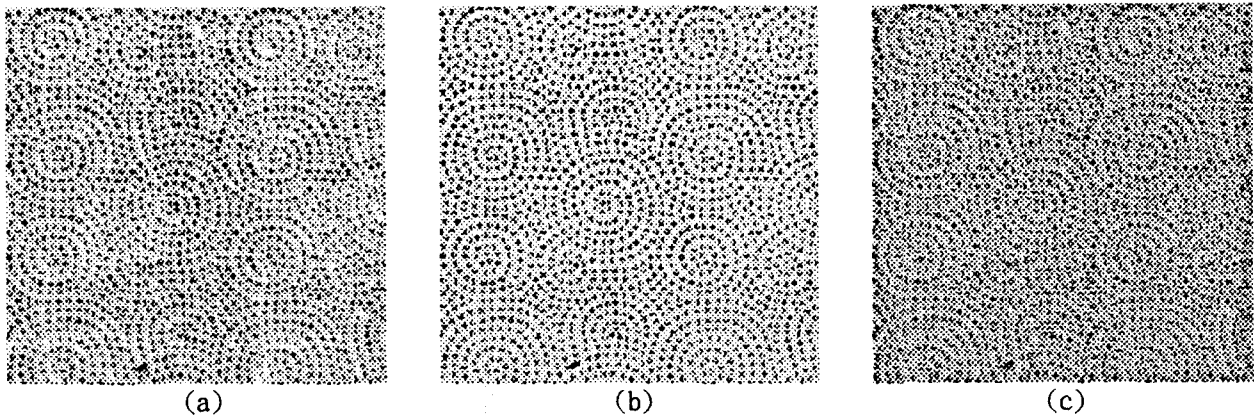


Fig. 2. Experimental results for **Case 1** associated with Example 2. (a) Blurred image; (b) the restored image obtained by the optimum inverse filter associated with $J_{2,3}$; (c) the restored image obtained by the 2-D correlation based prediction error method. (The original image is the one shown in Figure 1(a).)

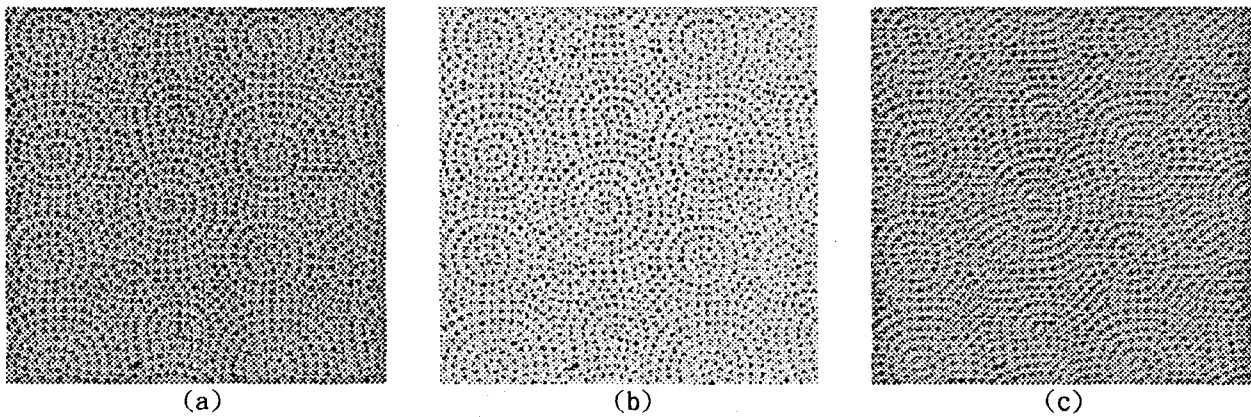


Fig. 3. Experimental results for **Case 2** associated with Example 2. (a) Blurred image; (b) the restored image obtained by the optimum inverse filter associated with $J_{2,3}$; (c) the restored image obtained by the 2-D correlation based prediction error method. (The original image is the one shown in Figure 1(a).)

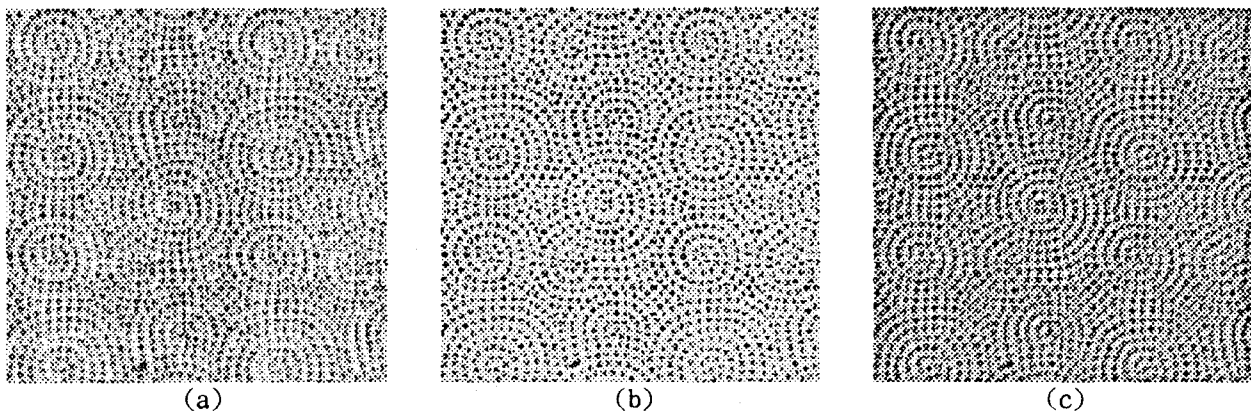


Fig. 4. Experimental results for **Case 3** associated with Example 2. (a) Blurred image; (b) the restored image obtained by the optimum inverse filter associated with $J_{2,3}$; (c) the restored image obtained by the 2-D correlation based prediction error method. (The original image is the one shown in Figure 1(a).)